CHAPTER 2

LITERATURE REVIEW

This chapter contains details on the brief description of necessary concepts that relate to the research i.e. ferroelectric properties, $BaTiO_3$ hysteresis measured by Sawyer-Tower experiment, Ising hysteresis generated by mean field calculation and Monte Carlo simulation, and Fourier transformation.

2.1 Ferroelectric properties and $BaTiO_3$

In crystallography, crystal structure can be primarily divided into 7 crystal systems which are cubic, tetragonal, orthorhombic, rhombohedral, hexagonal, monoclinic and triclinic. Further, these can be further classified into 32 point groups according to their crystallographic symmetry. However, only 21 point groups do not have a center of symmetry. Of these 21 point groups, 20 point groups correspond to materials which have the properties that an applied mechanical stress (on the materials) produces an electric field or on the other hand an electric field produces a mechanical stress. Such materials can be referred to as “piezoelectric” materials. In addition, these 20 piezoelectric materials can be subdivided into 10 sub-materials that have spontaneous polarization or electrical polarity. These polar groups have the property that the change in temperature induces an electric field. Such materials are called “pyroelectric” materials. A subset of these pyroelectric can have their spontaneous polarization reversed or enhanced by the application of a high enough electric field. This subset of the pyroelectric is the “ferroelectric” materials. The classification of the crystal structures showing the division into piezoelectric,

pyroelectric and ferroelectric can be shown in Fig. 2.1.

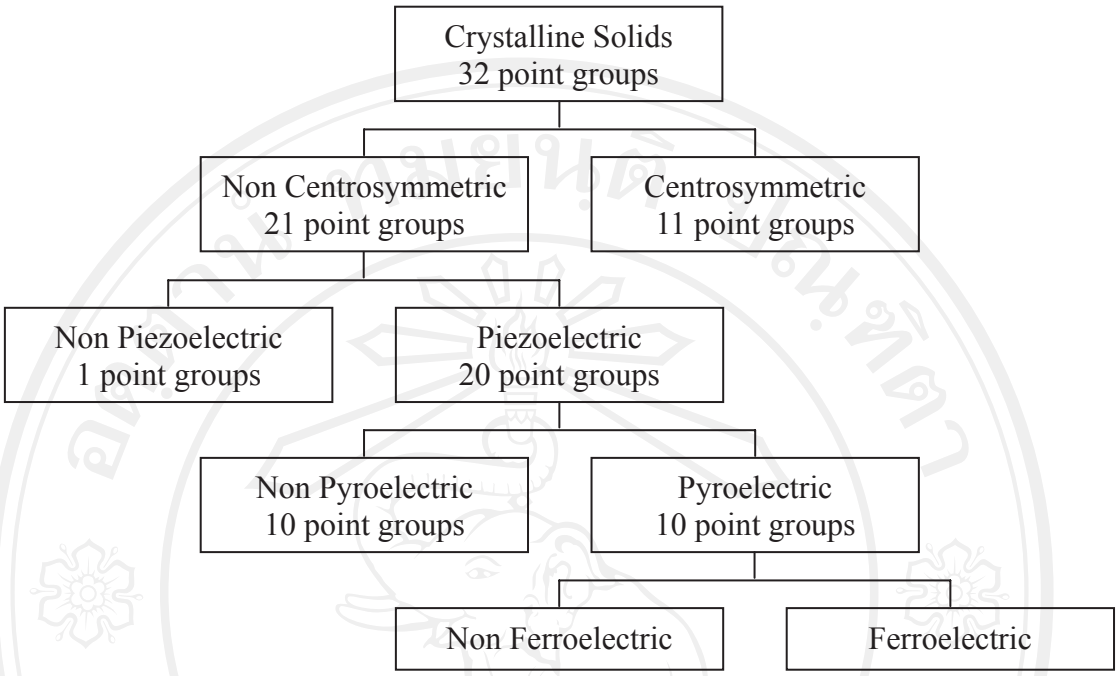

Figure 2.1 The classification of crystal structures showing the division into piezoelectric, pyroelectric and ferroelectric materials (modified from [18]).

Ferroelectric materials generally have transition temperature called the Curie point, T_C. At this Curie point, the material gets transformed from ferroelectric to paraelectric phases (see Fig. 2.2) as indicated by rapid decrease in the dielectric constant with increasing temperature. Above T_C, the material is in cubic structure and in paraelectric phase. In the paraelectric phase, the center of positive charge of the crystal coincides with the center of negative charge. As a result, the spontaneous polarization ceases. However, below T_C, the material is in ferroelectric phase where the center of positive and the center of negative charges are not at the same place. Therefore, the spontaneous polarization, i.e. the dipole moment per unit volume or the charge per unit area along the spontaneous polarization axis, is then developed. Additionally, this spontaneous polarization can be switched with electric field.

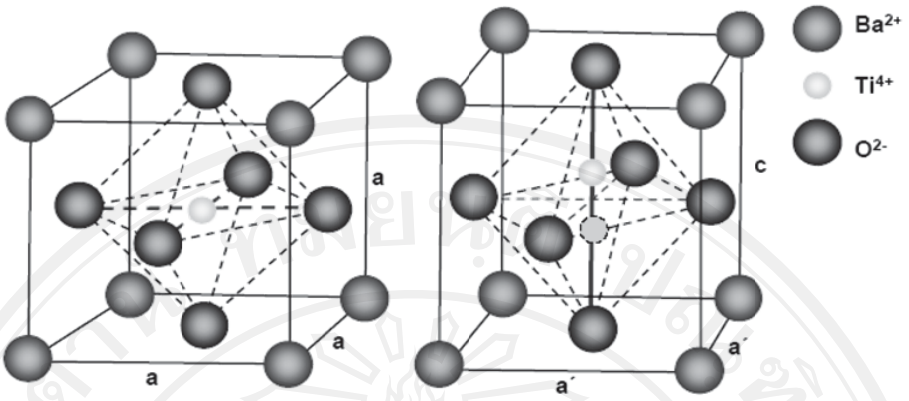

(a) $T > T_C$ (b) $T < T_C$

Figure 2.2 The transition between paraelectric (a) and ferroelectric (b) phases [19].

The plot of polarization versus electric field for the ferroelectric results in hysteresis loop as shown in Fig 2.3. The loop is generally non-linear so the polarization does not instantly response to electric field. For ferroelectric with zero spontaneous polarization, where the polarization from different domains cancel, the polarization increases with increasing the electric field until it arrives in its saturated level. This polarization level is called saturated polarization P_s. On the other hand, if the electric field decreases, the polarization also decreases. In such the case, even the electric field is zero, the ferroelectric crystal may still exhibit spontaneous polarization. The polarization that remains at the absence of electric field is called remnant polarization P_r. This remnant polarization can be removed when the applied electric field is large enough in the opposite direction. The magnitude of electric field that is required to cancel the remnant polarization is called the coercive field E_c.

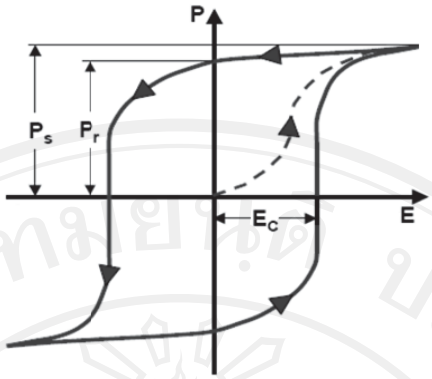

Figure 2.3 Typical ferroelectric hysteresis loop [20].

Presently, there are many important ferroelectric materials. To name a few are barium titanate ($BaTiO_3$, BT), lead titanate ($PbTiO_3$, PT), lead zirconate titanate (PZT), lead lanthanum zirconate titanate (PLZT), lead magnesium niobate (PMN) and potassium niobate ($KNbO_3$), etc. Although BT is not with the best electrical properties in comparison to Pb-based ferroelectric, the Pb-free BT ferroelectric has gained an intense interest due to eco-problem. In general, BT also has relatively high dielectric constant which may suit capacitor applications and piezoelectric transducer devices. In general, BT can be prepared from chemical reaction between barium oxide (BaO) and titanium dioxide (TiO_2), which forms a perovskite structure as shown in Fig. 2.4.

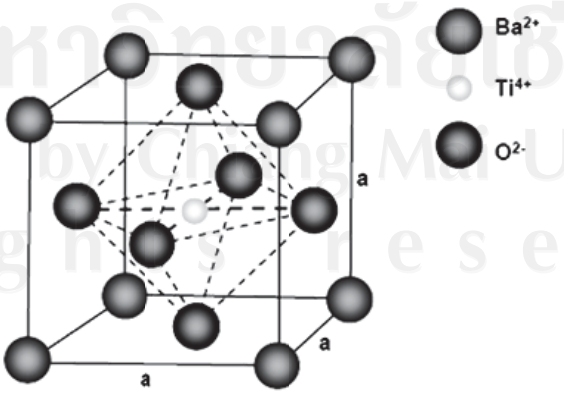

Figure 2.4 Perovskite structure of $BaTiO_3$ [19].

With increasing temperature, the BT crystal structure changes (see Fig. 2.5). To specify, BT crystal structure is rhombohedral when temperature is lower than -90 °C, orthorhombic when temperature is between 90 to 0 °C and tetragonal when temperature is between 0 to 130 °C. If temperature is above 130 °C (which is the Curie temperature, T_C), BT changes to paraelectric where and the crystal structure is cubic.

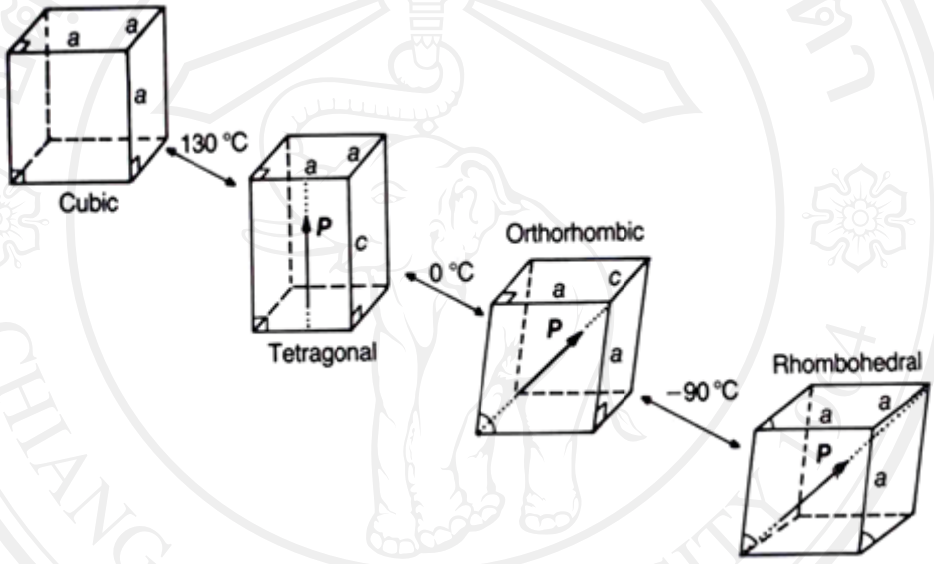

Figure 2.5 The temperature dependent crystal structure of $BaTiO_3$ [21].

2.2 Ferroelectric hysteresis measurement

Ferroelectric hysteresis can be measured using Sawyer-Tower circuit (see Fig. 2.6). In measuring, the ferroelectric sample is inserted between parallel plates to form capacitor C_S (sample capacitance) which connect in series to a reference capacitor C_0 (reference capacitance). An exact equivalent circuit, made from the series resistors of R_1 and R_2, is then connected in parallel to the series capacitors, where R_1 is preferably to be much higher than R_2.

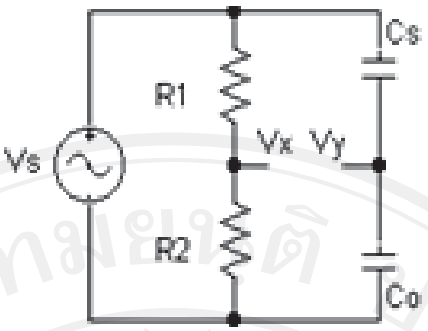

Figure 2.6 Sawyer-Tower circuit [22, 23].

In the circuit, V_x is the voltage across R_2 which is assumed to be equal to C_S. Therefore, the electric field can be obtained from

$$E = \frac{V_x}{d}. \tag{2.1}$$

Additionally, due to the connection of C_S and C_0 in series, the electric charges Q on each capacitor are also equal. Since, $Q = CV$, the voltage across C_0 is V_y therefore polarization can be calculated from

$$P = \frac{C_0 V_y}{A}, \tag{2.2}$$

where d and A are the thickness and area of ferroelectric sample, respectively. From Eq. (2.1) and (2.2), ferroelectric hysteresis can then be obtained. Additionally, ferroelectric hysteresis can be obtained from the mathematical system i.e. Ising model.

2.3 Ising model

Ising model is the mathematical system having only two possible states [24-27]. Therefore, it can be used to model very strong anisotropic ferroelectric system having only two possible directions of molecular dipole moments. In the Ising model,

the molecular dipole moment is called Ising dipole moment, where each Ising dipole moment interacts only with its neighboring dipoles as shown in Fig. 2.7.

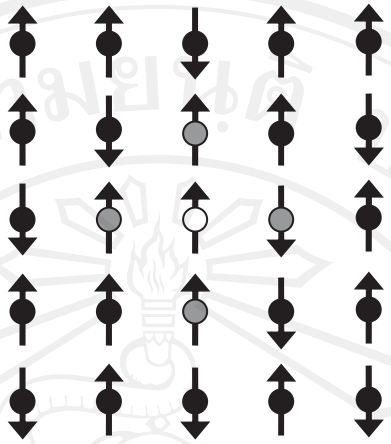

Figure 2.7 Ising dipole moments configuration, where each Ising dipole moment u_i (white) interacts mostly with its nearest neighbors u_j (gray).

The Hamiltonian of Ising model under the presence of external field has a form

$$H = -\frac{1}{2}\sum_{\langle i,j\rangle} J_{ij} u_i u_j - \sum_i E_i u_i \,, \tag{2.3}$$

where $-\frac{1}{2}\sum_{\langle i,j\rangle} J_{ij} u_i u_j$ is the interaction between Ising dipole moment u_i and its nearest neighboring u_j, the symbol $< >$ indicates that only neighboring is considered in the sum, and $-\sum_i E_i u_i$ is the interaction between electric field and Ising dipole moment u_i. In term of the exchange interaction J_{ij}, the model can represents ferroelectric behavior in nature. For example, if $J_{ij} > 0$ the system presents ferroelectric state while if $J_{ij} < 0$ the system presents anti-ferroelectric state. Ising hysteresis can be generated from mean field calculation and Monte Carlo simulation.

2.4 Mean field theory

In mean field theory, it is assumed that each local polarization can be calculated from the average of all molecular dipole moments in the system where fluctuations can be neglected i.e.

$$P = \frac{1}{N}\left\langle \sum_{i=1}^{N} u_i \right\rangle, \tag{2.4}$$

where N is the number of molecules. From the Ising Hamiltonian, the mean field writes

$$\begin{aligned} u_i u_j &= (u_i - P + P)(u_j - P + P) \\ &= P^2 + P(u_i - P) + P(u_j - P) + (u_i - P)(u_j - P), \end{aligned} \tag{2.5}$$

where fluctuations term $(u_i - P)(u_j - P)$ is discarded and $u_i u_j$ is fed back into Eq. (2.3). Then the Ising Hamiltonian can be rewritten as

$$H = -\frac{1}{2}\sum_{\langle i,j \rangle} J_{ij}[-P^2 + P(u_i + u_j)] - \sum_i E_i u_i \,. \tag{2.6}$$

The exchange interaction is further assumed that $\sum_j J_{ij} = z\tilde{J} = J$, where z is the number of nearest neighbor of each molecular dipole moment. Therefore, $\sum_{\langle i,j \rangle} J_{ij} = NJ$ and Eq. (2.6) becomes

$$H = \frac{1}{2}JNP^2 - [E + JP)]\sum_i u_i \,. \tag{2.7}$$

In addition, the partition function takes a form

$$Z_i = e^{\frac{1}{2}\beta JNP^2} \sum_i e^{\beta(JP+E)u_i} = e^{\frac{1}{2}\beta JNP^2}(e^x + e^{-x}) = e^{\frac{1}{2}\beta JNP^2}\, 2\cosh(x)\,, \tag{2.8}$$

where $x = \beta(JP + E)$, $\beta = 1/k_B T$ and k_B is Boltzmann's constant. Polarization can be found from expectation value $P = \sum_i \mu_i p(u_i)$, where $u_i = \pm 1$ and $p(u_i)$ is Boltzmann probability, i.e.

$$\begin{aligned} P &= 1P_{\uparrow} + (-1)p_{\downarrow} = \frac{e^{\frac{1}{2}\beta JNP^2}}{Z_i}(e^x - e^{-x}) = \tanh(x) \\ &= \tanh[\beta(JP + E)] \end{aligned} . \tag{2.9}$$

From Eq. (2.9), it is implied that mean field theory can be used to extract polarization under effect of electric field.

2.4.1 Dynamic mean field equation

Mean field theory can also be used to extract polarization under effect of time dependent electric field, called the dynamic mean field equation. From master equation [28],

$$\begin{aligned} \frac{dP(u_1,...,u_i,...,u_N:t)}{dt} &= -\sum_i W_i(u_i)P(u_1,...,u_i,...,u_N:t) \\ &\quad + \sum_i W_i(-u_i)P(u_1,...,-u_i,...,u_N:t), \end{aligned} \tag{2.10}$$

where $P(u_1,...,u_i,...,u_N:t)$ is the probability in changing molecular dipole moment configuration $(u_1,...,u_i,...,u_N)$ and $W_i(u_i)$ is the probability in finding molecular dipole moment at the u_i state. In equilibrium state, $\frac{dP(u_1,...,u_i,...,u_N:t)}{dt} = 0$, Eq. (2.10) becomes

$$W_i(u_i)P(u_1,...,u_i,...,u_N:t) = W_i(-u_i)P(u_1,...,-u_i,...,u_N:t). \tag{2.11}$$

Replacing $P(u_1,...,u_i,...,u_N)$ with Boltzmann probability into Eq. (2.11), it leads to

$$\frac{W_i(u_i)}{W_i(-u_i)} = \frac{e^{-\beta H_i u_i}}{e^{\beta H_i u_i}}, \tag{2.12}$$

where $H_i = \sum_j J_{ij}\mu_j + E_i$ is local field. As $e^x = 1 + x + \frac{x^2}{2!} + \frac{x^3}{3!} + \ldots$, Eq. (2.12) gives

$$W_i(u_i) = \frac{1}{2\tau}(1 - u_i \tanh \beta H_i), \tag{2.13}$$

where τ depends on temperature and other dipole moments. The average of dipole moments is given by

$$\langle u_i \rangle = \sum_i u_i P(u_1,...,u_i,...,u_N). \tag{2.14}$$

Multiplication u_i and replacing $W_i(u_i)$ and $\langle u_i \rangle$ into Eq. 2.10, it gives

$$\tau \frac{d\langle u_i \rangle}{dt} = -\langle u_i \rangle + \tanh \beta \langle H_i \rangle, \tag{2.15}$$

where $\langle H_i \rangle = \sum_j J_{ij} \langle \mu_j \rangle + E_i$. Since polarization can be calculated from the average of all molecular dipole moments in the system, Eq. (2.15) becomes

$$\tau \frac{dP(t)}{dt} = -P(t) + \tanh \beta \left(E(t) + \sum_j J_j P(t) \right). \tag{2.16}$$

2.5 Monte Carlo simulation

Monte Carlo simulation [29] is generally used to simulate the random thermal fluctuation of the system in changing from state to state and calculate the expectation value of the observable quantities. The advantage of this technique is that it requires only a small fraction of states of the system to get accurate estimates of physics quantities. Monte Carlo simulation contains important principles that are important sampling, Markov process and Metropolis algorithm.

2.5.1 Important sampling

The expectation value $\langle Q \rangle$ can be calculated from averaging the observable quantity Q over all states μ in the system, weighting each with its Boltzmann probability,

$$\langle Q \rangle = \frac{\sum_{\mu} Q_{\mu} \exp\left(-E_{\mu}/k_B T\right)}{\sum_{\mu} \exp\left(-E_{\mu}/k_B T\right)}. \tag{2.17}$$

This is tractable in the very small systems, but in the large systems, the expectation value $\langle Q \rangle$ has to be estimated from the averaging of the observable quantity Q over M subset of important states μ in the system. This M subset of important states μ can be chosen according to the probability $p_{\mu} = Z^{-1} \exp\left(-E_{\mu}/k_B T\right)$. In general, the estimable $\langle Q \rangle$ is given by

$$Q_M = \frac{\sum_{i=1}^{M} Q_{\mu_i} p_{\mu_i}^{-1} \exp\left(-E_{\mu_i}/k_B T\right)}{\sum_{i=1}^{M} p_{\mu_i}^{-1} \exp\left(-E_{\mu_i}/k_B T\right)}, \tag{2.18}$$

where Q_M is called the estimator of $\langle Q \rangle$. It has the property that, if the number of M subset of important states μ increase, $Q_M \to \langle Q \rangle$ when $M \to \infty$. Notice that the Boltzmann factors cancel and the estimator of $\langle Q \rangle$ becomes

$$Q_M = \frac{1}{M} \sum_{i=1}^{M} Q_{\mu_i}. \tag{2.19}$$

2.5.2 Markov process

Markov process is a mechanism which generated new state ν from a given

state μ. The probability for transition from state μ to state ν is called the transition probability $P(\mu \to \nu)$ which must also satisfy the constraint,

$$\sum_{\nu} P(\mu \to \nu) = 1. \tag{2.20}$$

Additionally, Markov process should satisfy two further conditions that is

- The condition of ergodicity: The transition probability between any two states must be non-zero.
- The condition of detailed balance: The transition rate into and out of any state μ must be equal i.e.

$$\frac{P(\mu \to \nu)}{P(\nu \to \mu)} = \frac{p_{\nu}}{p_{\mu}} = \exp\left(\frac{-(E_{\nu} - E_{\mu})}{k_B T}\right). \tag{2.21}$$

In general, Markov process decomposes the transition probability down into two parts

$$P(\mu \to \nu) = g(\mu \to \nu) A(\mu \to \nu). \tag{2.22}$$

In Eq. (2.22), $g(\mu \to \nu)$ is the selection probability to generate new state ν from given state μ, and $A(\mu \to \nu)$ is the acceptance probability to accept the new state ν from given state μ

$$\frac{P(\mu \to \nu)}{P(\nu \to \mu)} = \frac{g(\mu \to \nu) A(\mu \to \nu)}{g(\nu \to \mu) A(\nu \to \mu)} = \exp\left(\frac{-(E_{\nu} - E_{\mu})}{k_B T}\right). \tag{2.23}$$

2.5.3 Metropolis algorithm

Metropolis algorithm is a method which considered the transition probability from given state μ to new state ν, where $g(\mu \to \nu)$ for each of the possible state ν is chosen to be equal. Suppose there are *N* possible states which can be reach from state μ. Each of the selection probabilities takes a form

$$g(\mu \to \nu) = g(\nu \to \mu) = \frac{1}{N}. \tag{2.24}$$

With these selection probabilities, Eq. (2.23), becomes

$$\frac{P(\mu \to \nu)}{P(\nu \to \mu)} = \frac{A(\mu \to \nu)}{A(\nu \to \mu)} = \exp\left(\frac{-(E_\nu - E_\mu)}{k_B T}\right). \tag{2.25}$$

Further, the Metropolis aims to push the system to its equilibrium state as fast as possible so the acceptance probability is set to

$$A(\mu \to \nu) = \begin{cases} \exp\left(\dfrac{-(E_\nu - E_\mu)}{k_B T}\right) & ; E_\nu - E_\mu > 0 \\ 1 & ; E_\nu - E_\mu \le 0. \end{cases} \tag{2.26}$$

2.6 Fourier transformation

The Fourier transformation is an operation that transforms the function in one domain into its corresponding inverse domain e.g. time domain into frequency domain. The Fourier transformation is a powerful technique in treating various problems involving the periodic function $f(t)$ with period T has a form

$$f(t) = f(t+T). \tag{2.27}$$

Additionally, this periodic function $f(t)$ can be represented in term of Fourier series which contains cosine and sine functions as

$$f(t) = \frac{1}{2}a_0 + \sum_{n=1}^{\infty}(a_n \cos 2\pi n f_0 t + b_n \sin 2\pi n f_0 t) \tag{2.28}$$

or

$$f(t) = \frac{1}{2}a_0 + \sum_{n=1}^{\infty} c_n \sin(2\pi n f_0 t - \varphi_n). \tag{2.29}$$

As can be seen, the periodic function $f(t)$ represents a sum of sinusoidal components having different frequency $f_n = nf_0$, the so called frequency of the n^{th} harmonic. Frequency of the 1^{th} harmonic f_1 is called fundamental frequency, because it has the same period as the function $T = 1/f_0$. The coefficients a_n and b_n are known as Fourier coefficients of n^{th} harmonic of the real and imaginary parts respectively, where the coefficients c_n and the angles $\varphi_n = \tan^{-1}(a_n / b_n)$ are denoted as Fourier coefficients of n^{th} harmonic and phase angles, respectively. There Fourier coefficients can be evaluated from

$$a_0 = \frac{2}{T}\int_{-T/2}^{T/2} f(t)dt \tag{2.30}$$

$$a_n = \frac{2}{T}\int_{-T/2}^{T/2} f(t)\cos(2\pi n f_0 t)dt \qquad n = 1, 2, 3, \ldots \tag{2.31}$$

$$b_n = \frac{2}{T}\int_{-T/2}^{T/2} f(t)\sin(2\pi n f_0 t)dt \qquad n = 1, 2, 3, \ldots \tag{2.32}$$

$$c_n = \frac{2}{T}\int_{-T/2}^{T/2} f(t)\sin(2\pi n f_0 t - \varphi_n)dt \qquad n = 1, 2, 3, \ldots \tag{2.33}$$

2.6.1 Continuous Fourier transformation

The continuous Fourier transformation can be used to transform the simple function that is integral. The forward Fourier transformation has a form

$$F(f) = \int_{-\infty}^{\infty} f(t)\exp(-i2\pi f t)dt\,. \tag{2.34}$$

In Eq. (2.34), the function in time domain can be transformed using integral operation into the corresponding function in frequency domain. On the other hand, the inverse Fourier Transformation has a form

$$f(t) = \int_{-\infty}^{\infty} F(f)\exp(i2\pi tf)df \,. \tag{2.35}$$

In Eq. (2.35), the function in frequency domain can be transformed by using integral operation back into the corresponding function in time domain.

2.6.2 Discrete Fourier transformation

The discrete Fourier transformation can be used to transform, instead of a function, the set of discrete data points. The forward discrete Fourier transformation has form

$$F(k) = \sum_{n=0}^{N-1} f(n)\exp(-i2\pi nk/N). \tag{2.36}$$

In Eq. (2.36), the set of data points in time domain can be transformed by using summation operator in finding corresponding set of data points in frequency domain. The inverse discrete Fourier Transformation has a form

$$f(n) = \frac{1}{N}\sum_{n=0}^{N-1} F(k)\exp(i2\pi nk/N). \tag{2.37}$$

In Eq. (2.37), the set of data points in frequency domain can be transformed by using another summation operator in finding corresponding set of data points in time domain, where N is number of data points per period. In the discrete Fourier transformation, the time intervals between data points need to be equal and the numbers of data points per period should be large enough for specifying the complicate function. The discrete Fourier transformation then requires much of computing resource, because it has the number of multiplications of complex number equal to N^2. The more efficient transformation is then be required treating the problems.

2.6.3 Fast Fourier transformation

The fast Fourier transformation is an efficient transformation that can decrease the number of multiplications of complex number (from N^2 to $N \log_2 N$) by dividing and rearranging data points into many small groups. After that, the discrete Fourier transform will be operated on the data in each group. Then, the transforming data points are combined into larger groups and re-transformed. The re-grouping and re-transforming go on until all data points merge to one group (with N data points). Therefore, the most suitable number of data points of the fast Fourier transformation should be equal to power of two (e.g. 2, 4, 8…).

From the discrete Fourier transformation, $W_N^{kn} = \exp(-2\pi kn / N)$ is substituted into Eq. (2.36),

$$F(k) = \sum_{n=0}^{N-1} f(n) W_N^{kn} . \tag{2.38}$$

According to linear property of the discrete Fourier transformation, $f(n)$ can be divided into 2 groups that is $f(2r)$ for even n and $f(2r+1)$ for odd n where $r = 0, 1, ..., N/2-1$. Therefore,

$$F(k) = \sum_{r=0}^{N/2-1} f(2r) W_N^{2kr} + \sum_{r=0}^{N/2-1} f(2r+1) W_N^{k(2r+1)}, \tag{2.39}$$

And

$$F(k) = \sum_{r=0}^{N/2-1} f(2r) W_{N/2}^{kr} + W_N^k \sum_{r=0}^{N/2-1} f(2r+1) W_{N/2}^{kr} . \tag{2.40}$$

The data points are then rearranged into new functions that is $g(r) = f(2r)$ and $h(r) = f(2r+1)$, and these lead to

$$F(k)=\sum_{r=0}^{N/2-1} g(r)W_{N/2}^{kr}+W_N^k\sum_{r=0}^{N/2-1} h(r)W_{N/2}^{kr}, \tag{2.41}$$

And

$$F(k)=G(k)+W_N^k H(k), \tag{2.42}$$

where $G(k)=\sum_{r=0}^{N/2-1} g(r)W_{N/2}^{kr}$ and $H(k)=\sum_{r=0}^{N/2-1} h(r)W_{N/2}^{kr}$. From 1 step of dividing and rearranging data points in to 2 groups, the number of multiplications of complex number can be specified as follows:

- The number of multiplications of $g(r)$ and $W_{N/2}^{kr}$ in $G(k)$ calculation = $(N/2)^2$
- The number of multiplications of $h(r)$ and $W_{N/2}^{kr}$ in $H(k)$ calculation = $(N/2)^2$
- The number of multiplications of $H(k)$ and W_N^k in $F(k)$ calculation = N

As a result, the number of multiplications of complex number therefore equal to $N+N^2/2<N^2$. The diagram of data points flowing into the fast Fourier transformation (butterfly diagram) by dividing and rearranging data points in 1 step for $N=8$ is shown in Fig. 2.8.

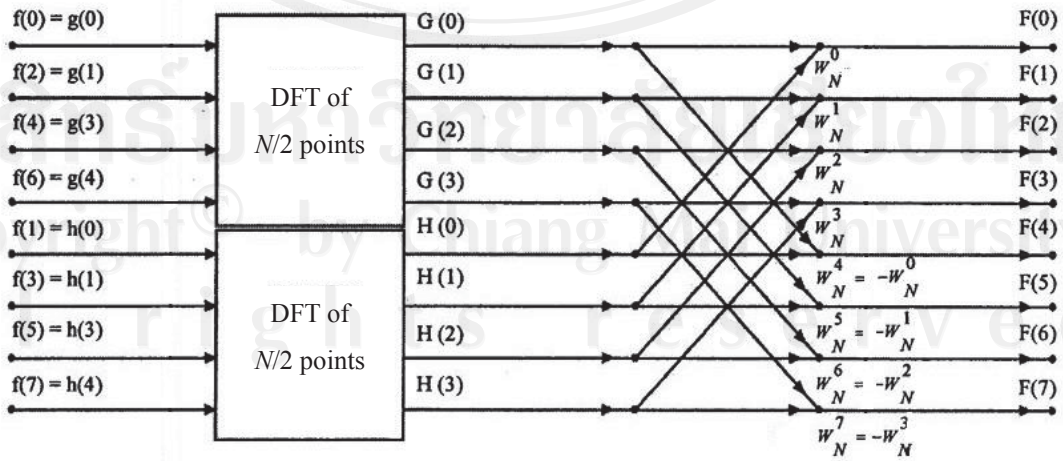

Figure 2.8 Butterfly diagram of the fast Fourier transformation by dividing and rearranging data points in 1 step for $N = 8$ (modified from [30]).

In explaining the butterfly diagram in Fig. 2.8 of $N/2$ is factorization of 2, $g(r)$ can be divided into 2 groups that is $g(2l)$ for even r and $g(2l+1)$ for odd r where $l = 0, 1, ..., N/4-1$ and $h(r)$ can be divided into 2 groups that is $h(2l)$ for even r and $h(2l+1)$ for odd r where $l = 0, 1, ..., N/4-1$, i.e.

$$G(k) = \sum_{l=0}^{N/4-1} g(2l) W_{N/2}^{2kr} + \sum_{r=0}^{N/4-1} g(2l+1) W_{N/2}^{k(2r+1)} \tag{2.43}$$

$$G(k) = \sum_{l=0}^{N/4-1} g(2l) W_{N/4}^{kr} + W_{N/2}^{k} \sum_{r=0}^{N/4-1} g(2l+1) W_{N/4}^{kr} \tag{2.44}$$

and

$$H(k) = \sum_{l=0}^{N/4-1} h(2l) W_{N/2}^{2kr} + \sum_{r=0}^{N/4-1} h(2l+1) W_{N/2}^{k(2r+1)} \tag{2.45}$$

$$H(k) = \sum_{l=0}^{N/4-1} h(2l) W_{N/4}^{kr} + W_{N/2}^{k} \sum_{r=0}^{N/4-1} h(2l+1) W_{N/4}^{kr} . \tag{2.46}$$

Then, with from 2 steps of dividing and rearranging data points into 4 groups, the number of multiplications of complex number is:

- The number of multiplications in $G(k)$ calculation = $N/2 + 2(N/4)^2$
- The number of multiplications in $H(k)$ calculation = $N/2 + 2(N/4)^2$
- The number of multiplications of $H(k)$ and W_N^k in $F(k)$ calculation = N

As can be seen, the number of multiplications of complex number therefore equal to $2N + N^2/4 < N + N^2/2 < N^2$. The diagram of data points flowing in the fast Fourier transformation (butterfly diagram) by dividing and rearranging data points in 2 steps for $N = 8$ as shown in Fig. 2.9.

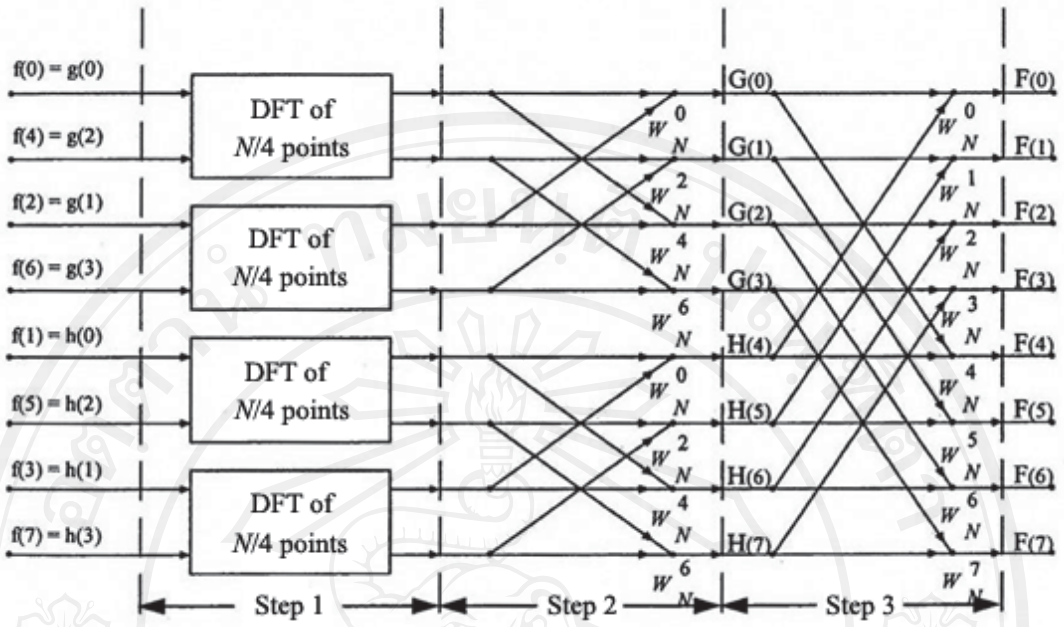

Figure 2.9 Butterfly diagram of the fast Fourier transformation by dividing and rearranging data points in 2 steps for $N = 8$ (modified from [30]).

Similarly, if $N/4$ is factorization of two, the small groups of data points will be divided and rearranged until the number of data points in each small groups are no longer be factorized. If the number of data points in each small group is $N/2^{\alpha}$ (α being the steps of dividing and rearranging data points), the number of multiplications of complex number therefore equal to $\alpha N + N^2/2^{\alpha} < \ldots < 2N + N^2/4 < N + N^2/2 < N^2$. In case of N is power of two ($N = 2^{\alpha}$ where α is integer), the number of multiplications of complex number therefore equal to $(\alpha - 1)2^{\alpha} + (2^{\alpha})^2/2^{\alpha} = \alpha 2^{\alpha}$ or $N \log_2 N$. As can be seen that the number of multiplications of complex number from the fast Fourier transformation much less than those from the direct discrete Fourier transformation especially where N is large as shown in Table 2.1.

Table 2.1 The number of multiplications of complex number comparison between the discrete Fourier transformation (DFT) and the fast Fourier transformation (FFT).

N	DFT N^2	FFT $N\log_2 N$
2	4	2
4	16	8
8	64	24
⋮	⋮	⋮
256	65,536	2,048
512	262,144	4,608
1,024	1,048,576	10,240